Supporting Material (SM): Contact, travel, & transmission

Contents

S1 Medical claims data

S1.1 Definition of ILI incidence ratio

We use the ILI incidence ratio as defined in [1]. Parameters referenced in the equation are described in Table S1.

$$\rho_{w,s} = (d_{w,s}/v_{w,s}) \times (p_s/100,000) \quad (1)$$

The incorporation of visits into this metric helps to account for artificialities in the medical claims data related to to physician office closures and changes to care-seeking behavior during the holidays, and increasing database coverage over time (Figure S1).

S1.2 Zip3 ILI incidence ratio during the holidays

We observed holiday-associated dips in the ILI incidence ratio at the zip3-level for each season (Figure S2).

S1.3 Estimation of the effective reproductive number

To understand the effect of the winter holidays on flu transmission in the empirical data, we estimated the effective reproductive number (R_t), the average number of secondary cases generated by each infected individual under the conditions at time t, over weekly periods during the eight flu seasons from 2001-2002 through 2008-2009. We used an estimated serial interval for flu of 3.6 days with a standard deviation of 1.6 days [2]. These analyses were performed with the EpiEstim package version 1.1-2 developed for the R programming language (R Foundation for Statistical Computing, Vienna, Austria) [3]. The EpiEstim data inputs were the U.S. weekly ILI medical claims, adjusted in two ways: 1) scaled up according to a ratio of total visits during a winter reference week to total visits during the reporting week, in order to account for temporal changes in healthcare-seeking behavior,

Figure S1: **Total visits to physicians reported by the medical claims dataset drops during holiday periods.** The grey bar highlights the typical school holiday for winter break, and a short dip (not highlighted) in late November demonstrates a similar pattern during the Thanksgiving holiday. Coverage in the medical claims dataset increases over time, as witnessed by the rising visit rates in each flu season.

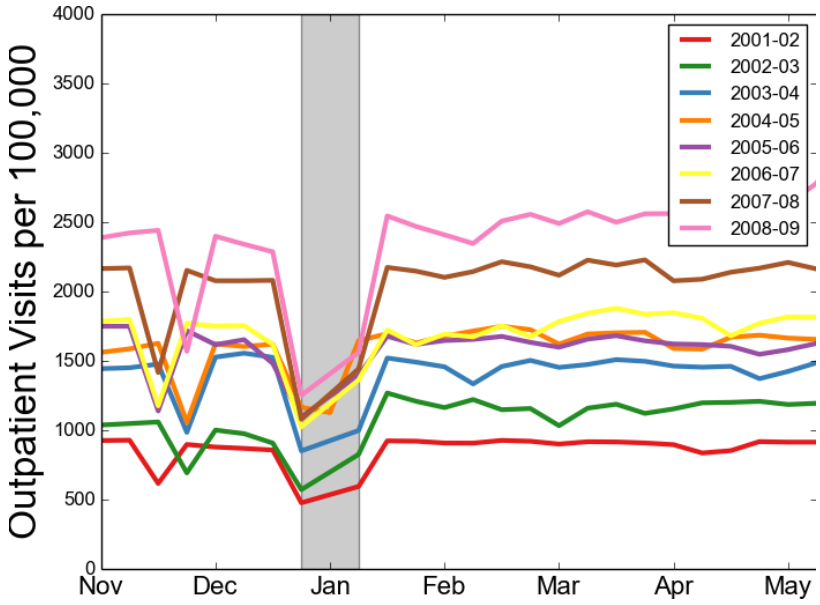

and 2) scaled up according to estimates that only 45% of the total population symptomatic with ILI seeks care from a physician (See SM section S1.3) [4, 5].

To account for changes in health care seeking behavior during holiday periods (Figure S1) and changes to medical claims coverage over time, we adjusted the raw ILI medical claims data for input into the EpiEstim program for estimation of the effective reproductive number R_t. Parameters referenced in the equation are described in Table S1.

$$d^*_{t,s} = (d_{w,s}/C) \times (v_{w_s}/v_{w,s}) \times (1/\phi) \tag{2}$$

S1.4 Verifying flu activity during the holidays

To examine whether ILI activity was due to influenza during the U.S. Thanksgiving and Christmas holidays, we used data that is publicly available from CDC's FluView Interactive application. These data were collected by the WHO/NREVSS Collaborating Labs and they represent the percentage of influenza-positive laboratory confirmations among all tested respiratory specimens in this CDC influenza surveillance system. We found that flu was regularly circulating by Christmas, but largely absent during the earlier Thanksgiving holidays (Figure S3A). During both holiday periods, thousands of samples were tested for influenza (Figure S3B).

S2 Metapopulation model

S2.1 Demographic and contact data

Spatial areas were modeled after metropolitan areas (236 areas were included, covering 79% of the U.S. population) as defined by the U.S. Bureau of Transportation Statistics. Each metropolitan area's population was divided into children (24%) and adults (76%), according to the national age distribution reported in the 2010 U.S. Census. Age-specific contact rates were adapted from a contact

Figure S2: **ILI incidence ratio during the holiday period for each study season at the zip3-level.** Each grey line represents the time series for a single zip3, and the dashed line indicates the week including Christmas.

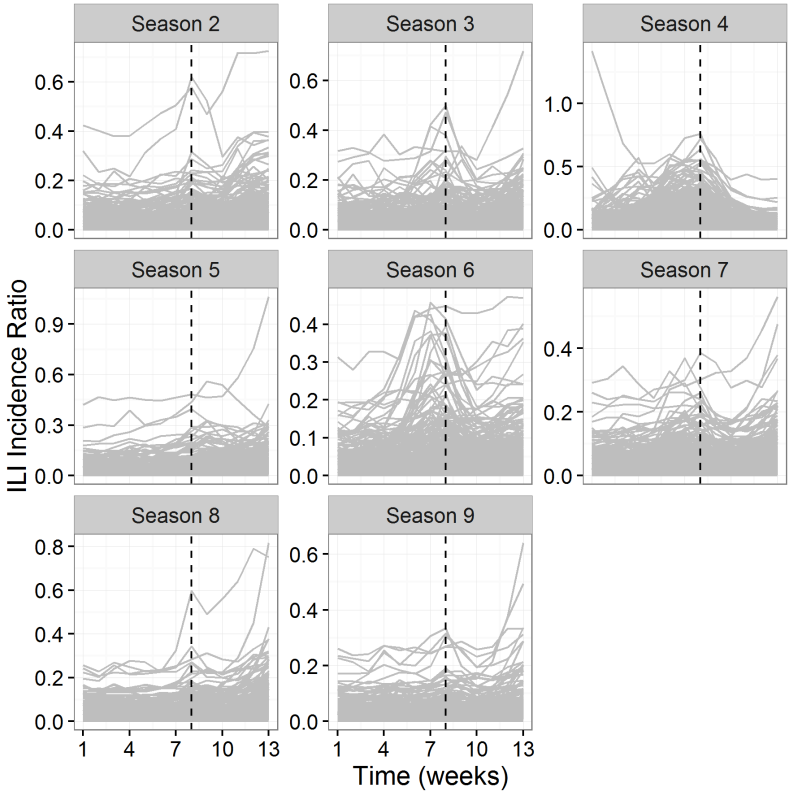

survey from Germany, given the similarity in demography to the United States [6], and translated to a contact matrix between children and adults (See SM section S2.1.1). Transmission parameters were chosen so that final epidemic sizes were 15-20% of the population [7], and the recovery rate corresponded to a two day infectious period, according to epidemiological survey data [8].

S2.1.1 Age-specific contact matrix

We utilize the following contact matrix structure where C_{cc} is the average number of daily contacts between children and C_{ac} is the average number of daily adult contacts reported by children, etc.

$$\begin{pmatrix} C_{cc} & C_{ca} \\ C_{ac} & C_{aa} \end{pmatrix}$$

Of the countries included in the study by Mossong et al ([6]), Germany represents a population most similar to the United States. Thus, we calculated the average number of daily contacts from German contact data using the following matrix, where q_c is the average number of child daily contacts weighted by German child population size, q_a is the average number of adult daily contacts weighted by German adult population size, p_c is the fraction of child daily contacts that occur with other children, p_a is the fraction of adult daily contacts that occur with other adults [6]. The parameter α is the fraction of the U.S. population represented by children [9].

$$\begin{pmatrix} p_c q_c/\alpha & (1-p_a)q_a/\alpha \\ (1-p_c)q_c/(1-\alpha) & p_a q_a/(1-\alpha) \end{pmatrix}$$

Age subgroups of children are indicated with subscript i (10-14, and 15-19 years old), age subgroups of adults are indicated with subscript j (20-24, 25-29, 30-34, 35-39, 40-44, 45-49, 50-54,

Table S1: **Parameters in adjustments to ILI medical claims data** The same notation was used to describe the ILI incidence ratio and the adjustments for the effective reproductive number analysis.

Common terms	
$d_{w,s}$	raw ILI cases at week w in season s
$v_{w,s}$	total visits to health care facilities for any diagnosis at week w in season s
Specific to equation 1	
$\rho_{w,s}$	ILI incidence ratio (IR) at week w in season s
p_s	population size in season s
Specific to equation 2	
$d^*_{t,s}$	adjusted ILI cases at day t in season s, input for effective reproductive number analysis
v_{w_s}	total visits to health care facilities for any diagnosis at winter reference week w_s
ϕ	estimate of the proportion of the total population that seeks care for symptomatic influenza-like illness (0.45)
Indicator variables	
w_s	winter reference week (chosen as the week of November 1 in a given season s)
t	indicator for time in days
s	indicator for flu season
w	indicator for time in weeks
C	number of days in a week (7 days)

Figure S3: **Flu activity is typically present during the Christmas holiday, but largely absent during the Thanksgiving holiday.** A) The percentage of influenza-positive laboratory confirmations over time, as collected from WHO/NREVSS, from the first week in November to the last week in January for flu seasons from 2001 to 2009. B) The number of samples tested for flu from WHO/NREVSS during the holiday period. The black dashed line represents the week of Christmas, and the grey dashed line represents the week of Thanksgiving.

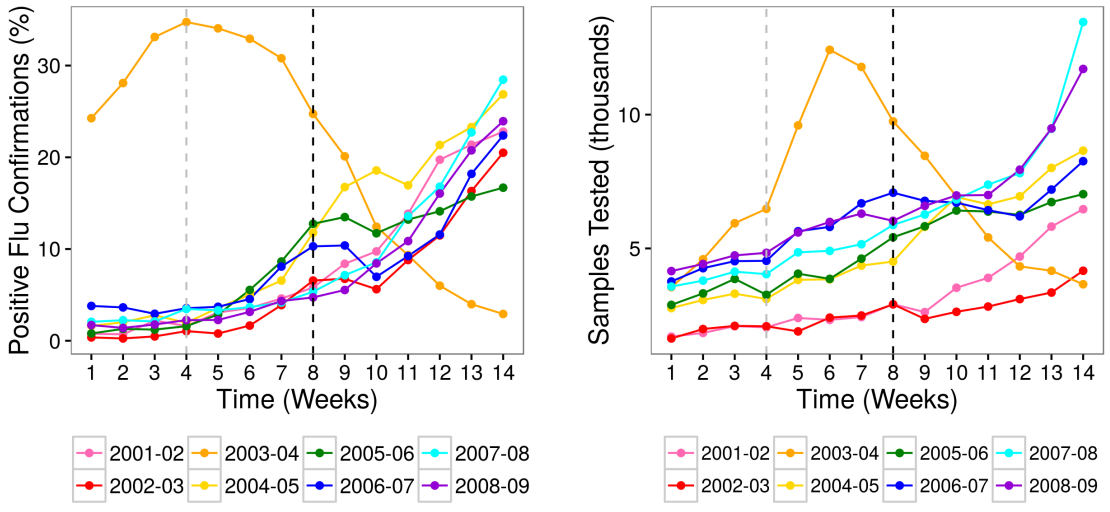

A) B)

55-59, 60-64, 65-69 years old). The average number of child daily contacts q_c and adult daily contacts q_a were calculated, where $x_{i,l}$ is the number of daily contacts between age subgroup i and all ages l, g_i or g_j is the population size of the age subgroup, g_c is the total child population size, and g_a is the total adult population size, and the number of subgroups for children and adults are denoted by N_i and N_j, respectively.

$$q_c = \sum_{i=1}^{N_i} (x_{i,l} \times g_i)/(g_c) \tag{3}$$

$$q_a = \sum_{j=1}^{N_j} (x_{j,l} \times g_j)/(g_a) \tag{4}$$

The fraction of child daily contacts that occur with other children p_c and the fraction of adult daily contacts that occur with other adults p_a were calculated as the ratio of the average number of within group contacts $r_{c/a}$ to the average number of total contacts $q_{c/a}$.

$$p_c = r_c/q_c \tag{5}$$

$$p_a = r_a/q_a \tag{6}$$

The average number of daily contacts that children had with other children r_c and that adults had with other adults r_a was calculated, where $x_{i,c}$ is the average number of daily contacts of child subgroup i with children c, and $x_{i,a}$ is the average number of daily contacts of adult subgroup i with adults a.

$$r_c = \sum_{i=1}^{N_i} (x_{i,c} \times g_i)/(g_c) \tag{7}$$

$$r_a = \sum_{j=1}^{N_j} (x_{j,a} \times g_j)/(g_a) \tag{8}$$

Given this structure, we present three contact matrices used in multiple analyses, in order: the non-holiday contact matrix, the full holiday contact matrix, and the partial contact matrix (SM only). https://preview.overleaf.com/public/hpxhpjpmcydy/images/b94044c2d2b779e0c798cf53093ef4c3851055cc.jpeg

$$\begin{pmatrix} 18.59 & 4.21 \\ 5.58 & 8.84 \end{pmatrix}$$

$$\begin{pmatrix} 7.78 & 2.55 \\ 5.83 & 8.15 \end{pmatrix}$$

$$\begin{pmatrix} 10.47 & 3.68 \\ 3.14 & 7.03 \end{pmatrix}$$

S2.2 Travel data

Travel movement rates were derived from domestic air traffic network data from the U.S. Bureau of Transportation Statistics from January to March 2005 (to represent baseline winter travel in the U.S.). The T100D Market Carriers table had data on the origin metropolitan area, the destination metropolitan area, and the average number of passengers traveling in a given month [10]. The average number of monthly passengers traveling between two metro areas i and j (in either direction), reported in the raw transportation data, was converted to the daily number of passengers w_{ij} traveling between two metro areas and used to determine travel flows between metro areas in the model at each time step. Travel rates were calculated separately for each age group and metro area pair i and j, by considering the population size and age breakdown of metro area i, the daily number of travelers between i and j w_{ij}, and the fraction of children who are travelers r. Children did not travel in the baseline model ($r = 0$), similar to previous studies [11, 9], because only 3% of travelers are children and less than 1% of trips made by children are greater than 30 miles during school term time [12].

S2.3 Holiday intervention period

The holiday period was chosen relative to the epidemic peak in the baseline model, based on the average duration from Christmas to the epidemic peak in the empirical data. The 14-day holiday period began 7 days before Christmas, and ended 7 days after Christmas to reflect the typical length of a winter break school holiday.

S2.4 Comparison of baseline and holiday air travel networks

We compared the baseline and holiday travel networks across common network measures for unweighted and weighted networks (Table S2). The baseline network represented average travel patterns from January to March 2005 (a typical winter period), the holiday network represented average travel patterns during December 2005 (a typical winter holiday period), and weights represented the average number of monthly passengers between two metro areas. The descriptive characteristics and unweighted network measures present the overall features and potential for connectivity, while the weighted network measures recast connectivity potential in the context of the volume of travel. The baseline network had a greater number of edges and larger average number of absolute connections (unweighted mean degree), while the holiday network had a greater maximum average number of passengers and larger passenger flows (weighted mean degree). This indicates that during the holidays, there is simultaneously a greater volume of travelers and a lower connectivity potential between airports, perhaps suggesting that this increased volume of holiday travelers seeks out fewer locations (e.g., holiday travelers flock to the largest cities). The holiday network appeared less right-skewed for the unweighted degree distribution and more right-skewed for the weighted degree distribution, corroborating the idea that the baseline network presented greater opportunities for connectivity between airports, but that the holiday network demonstrated an overall greater volume of travel (Figure S4).

These patterns were corroborated in examining differences between holiday and baseline network unweighted and weighted degrees (Figure S5), but differences between urban and rural connectivity during winter baseline and holiday periods may be obscured by the undirected nature of our network edge weights.

Airports had many fewer unique airport connections (unweighted degree) during holidays but similar or greater numbers of passengers (weighted degree) flowing through those airports. Notably, in comparing Figure S5A and Figure S5B, all of the decreases in unique airport connections were observed in small and medium sized cities, while airports in populous cities maintained similar numbers of flight connections during the holidays.

Table S2: **Comparison of baseline and holiday air travel networks across network measures.**

	Baseline	Holiday
Descriptive characteristics		
Number of nodes	228	225
Number of edges	4,189	3,187
Maximum of the average number of monthly passengers between two destinations	7,276,232	7,586,460
Unweighted measures		
Mean degree	36.75	28.33
Transitivity	0.54	0.50
Average clustering coefficient	0.61	0.62
Average shortest path length	2.03	2.11
Weighted measures		
Mean degree	4,904,132	5,106,540
Average clustering coefficient	0.0041	0.0067
Average shortest path length	5,689	14,232

Figure S4: **The holiday air travel network had fewer potential connections and a greater volume of travel than the winter baseline travel network.** A) The unweighted degree distribution appeared more right-skewed for the baseline network, while B) the weighted degree distribution appeared more right-skewed for the holiday network. The black vertical line in each figure represents the unweighted or weighted mean degree, as appropriate.

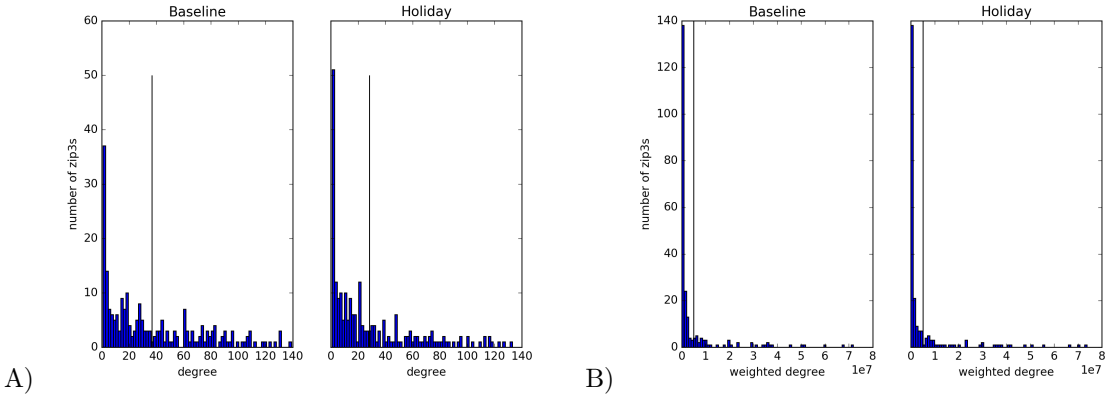

Figure S5: **The holiday air travel network experienced increased volume of travelers across similar or fewer unique airport connections.** Baseline network weighted and unweighted degrees were subtracted from holiday network weighted and unweighted degrees to represent the difference in weighted and unweighted degree metrics, respectively. A) Airports tended to have fewer unique connections during the holiday period (difference in unweighted degree) while maintaining similar numbers of passenger throughput (difference in weighted degree). B) In comparing difference in unweighted degree to population, decreases in unique airport connections were observed in small and medium sized cities, while airports in populous cities maintained similar numbers of flight connections during the holidays.

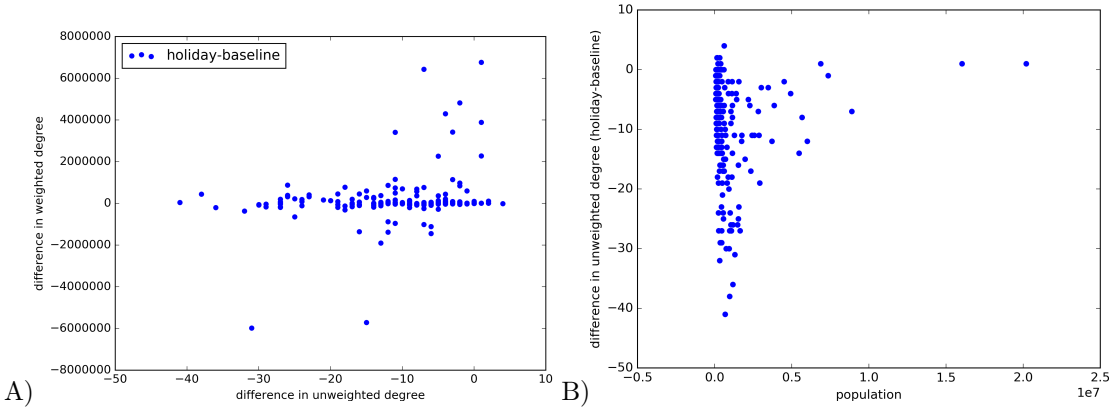

S3 Sensitivity Analysis of Model Results

S3.1 Contribution of contact reduction vs. assortativity to holiday changes

We acknowledge that the contact component of our model's holiday intervention combines two changes: 1) an overall reduction in contact rate, and 2) a change in the relative proportion of mixing between age groups. Here, we compare the baseline and main text contact intervention results (here, called 'full school closure') with simulations that reduced the age-specific number of contacts

but kept assortative mixing among age groups the same as that in the non-holiday contact matrix ('partial school closure') (Figure S6).

Figure S6: **A)** Total flu incidence per 10,000 population over time, averaged across all simulations. **B)** Distribution of time steps to peak across all metro areas, averaged across all simulations. **C)** Distributions of flu incidence across all metro areas averaged for the two week durations defined as 'before', 'during', and 'after' the holiday periods, averaged across all simulations. Distributions across metros are compared for the baseline, age-specific reduction in number of contact (partial school closure), and the main text contact only intervention (full school closure) simulations. The intervention period is demarcated by black dashed lines, as appropriate.

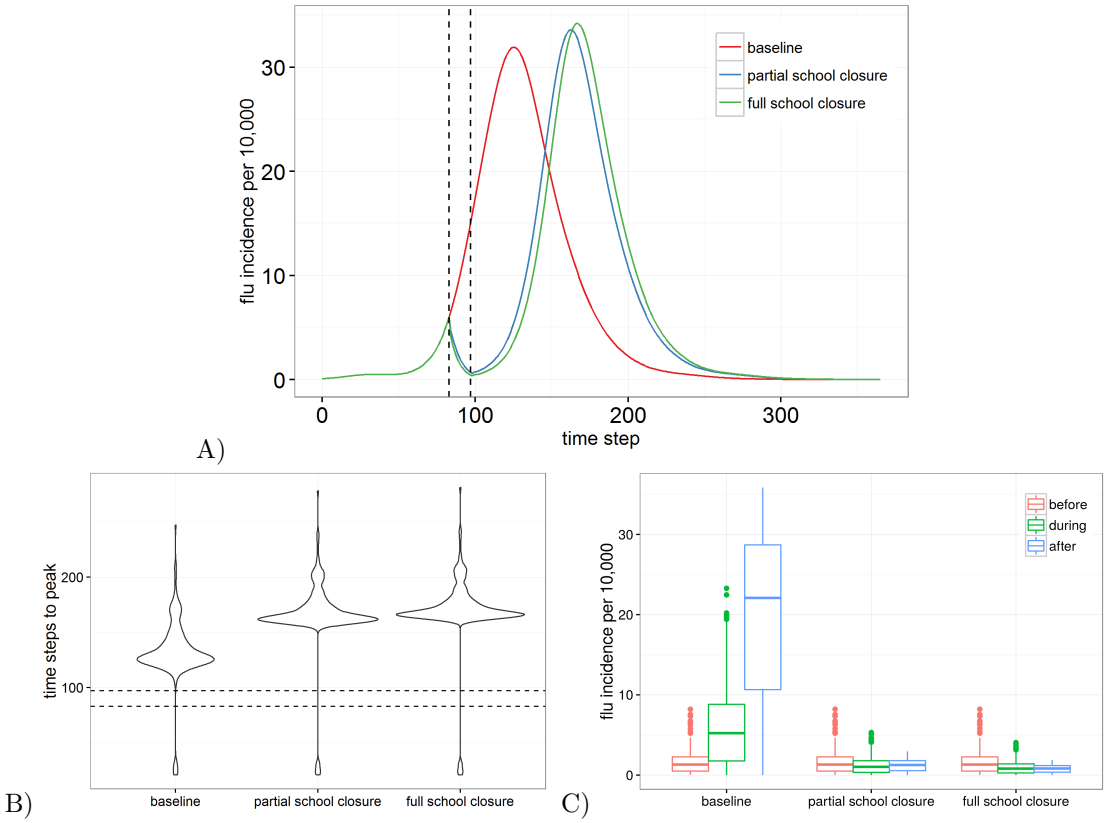

S3.2 Sensitivity of epidemic outcomes to contact reduction

We examined the sensitivity of epidemic outcomes to overall reductions in contact rate (called 'partial school closure' in Section S3.1). Two additional sets of simulations were performed, and relative to the original partial school closure simulations ('partial school closure'), they represented: 1) a 10% greater reduction in age-specific contacts ('-10% contact rate') and 2) a 10% smaller reduction in age-specific contacts ('+10% contact rate'). With larger contact rates (+10% contact rate), incidence peaks were earlier and smaller in magnitude. Synchrony was greater during the holiday period with lower contact rates than with higher contact rates, as represented with the narrower flu incidence distribution (Figure S7).

S3.3 Sensitivity of epidemic outcomes to holiday timing

We examined the sensitivity of model outcomes to holiday timings shifted three weeks ('+3 weeks') and six weeks ('+6 weeks') forward relative to the holiday timing presented in the main text ('actual'). The holiday reduced flu incidence to low levels (Figure S8) and shifted relative risk of disease

Figure S7: **A)** Total flu incidence per 10,000 population over time, averaged across all simulations. **B)** Distribution of time steps to peak across all metro areas, averaged across all simulations. **C)** Distributions of flu prevalence across all metro areas averaged for the two week durations defined as 'before', 'during', and 'after' the holiday periods, averaged across all simulations. Distributions across metros are compared for partial school closure, and 10% greater reduction (-10% contacts) and 10% smaller reduction (+10% contacts) in age-specific number of contacts. The intervention period is demarcated by black dashed lines, as appropriate.

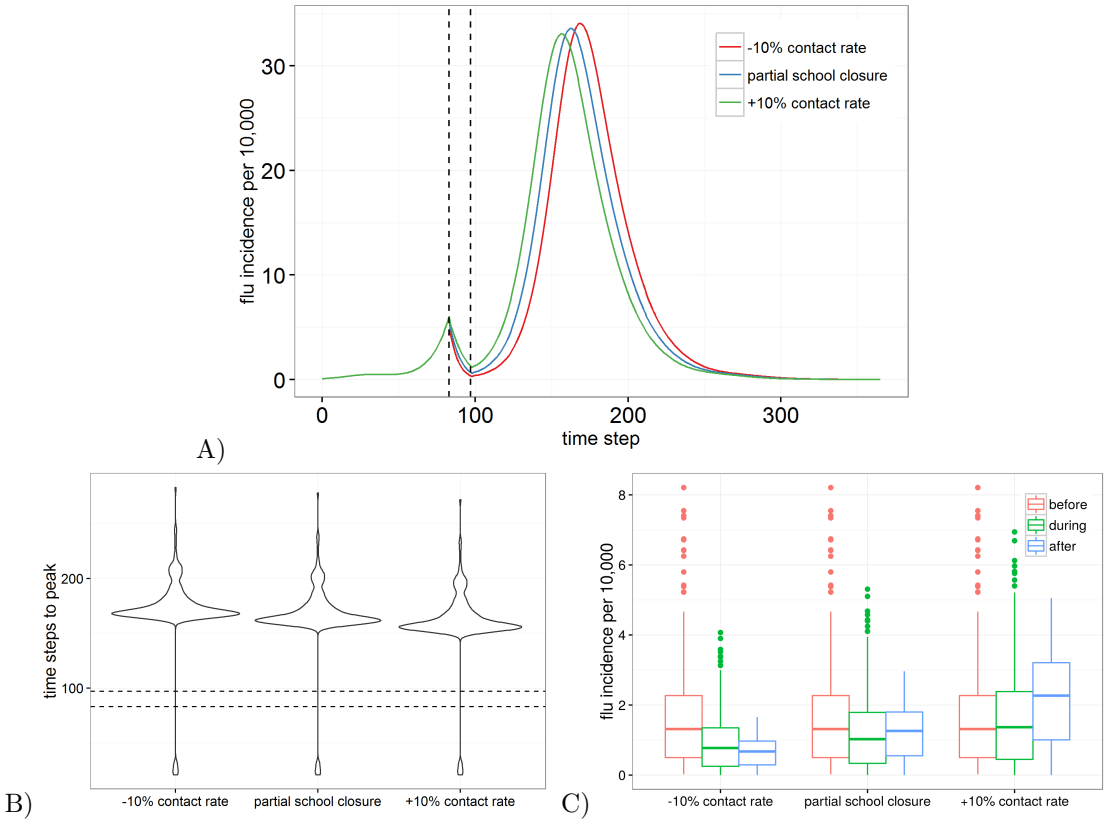

from children to adults (Figure S9) consistently across various holiday timings. Compared to the actual holiday simulations, peak timing was delayed for most locations in the +3 weeks simulations, and only for some locations in the +6 weeks simulations (Figure S10). While we expect holidays to delay epidemic peaks, many locations had already peaked by the time of the holiday in the +6 weeks simulations. Similarly, holidays consistently damped flu incidence and increase spatial synchrony across different timings, but the magnitude of recovery during the 'after' holiday period depended on the remaining susceptibility of the population (Figure S11).

Table S3: Percentage infected out of the total population, averaged across simulations.

Holiday Timing	Baseline	Travel	(Full) School Closure	Partial School Closure	Holiday
No holiday	18.28	-	-	-	-
Actual	-	18.32	17.68	17.67	17.73
+3 weeks	-	18.26	16.02	-	15.96
+6 weeks	-	18.29	14.92	-	14.89

Figure S8: **A)** Total flu incidence per 10,000 population over time, averaged across all simulations for holiday periods shifted forward by **A)** three weeks and **B)** six weeks. Epidemic trajectories for the baseline (no changes during intervention period), travel only, school closure only, and full holiday (travel and school closure changes) interventions are compared, and the intervention period is demarcated by the dashed black lines.

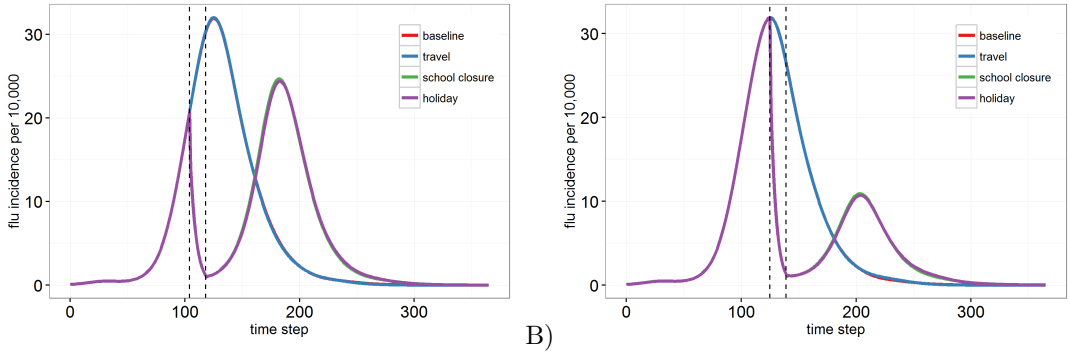

Figure S9: Relative risk of disease from children to adults across all locations, averaged across all simulations, for holiday periods shifted forward by **A)** three weeks and **B)** six weeks. Epidemic trajectories for the baseline (no changes during intervention period), travel only, school closure only, and full holiday (travel and school closure changes) interventions are compared, and the intervention period is demarcated by the dashed black lines.

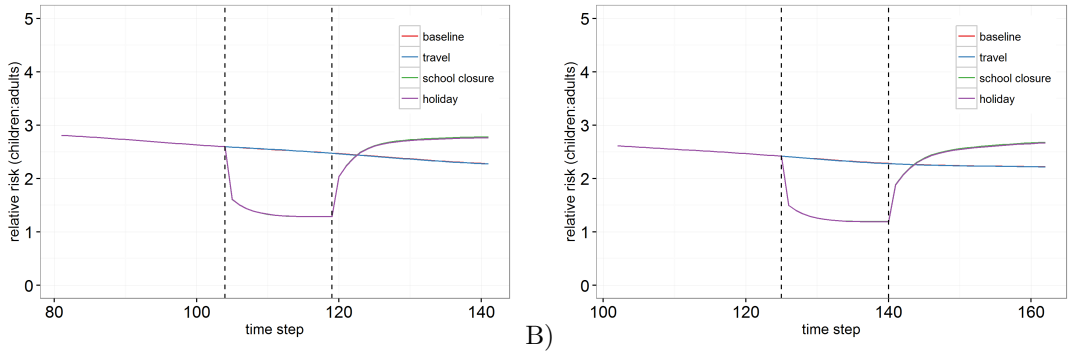

Figure S10: **A)** Distribution of time steps to peak across all metro areas, averaged across all simulations for holiday periods shifted forward by **A)** three weeks and **B)** six weeks. Distributions across metros are compared for the baseline, travel only, school closure only, and full holiday interventions, and the intervention period is demarcated by the dashed black lines.

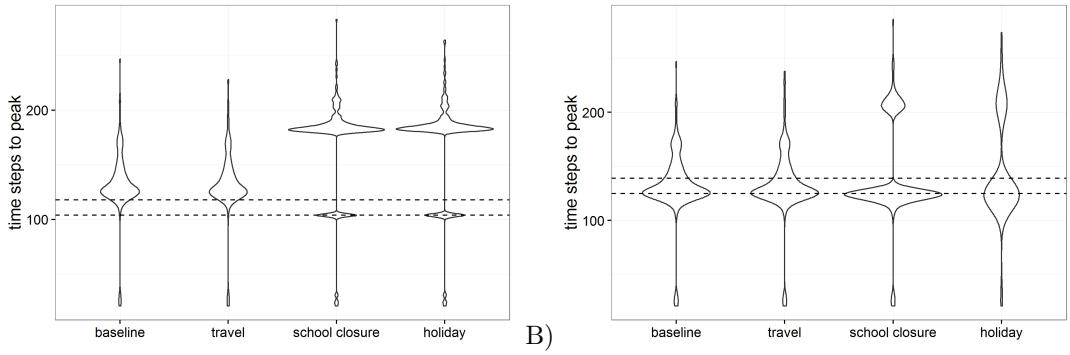

Figure S11: Distributions of flu prevalence across all metro areas averaged for the two week durations defined as 'before,' 'during,' and 'after' the holiday periods for three holiday intervention (travel and school closure) timings, averaged across all simulations.

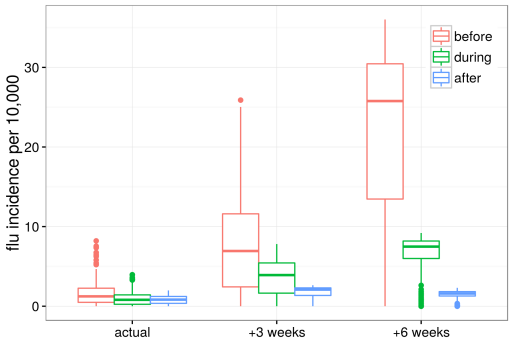

S3.4 Data access

Simulation code and model outputs averaged across all seeds for all intervention combinations and holiday timings will be made available at `https://github.com/bansallab`.

References

[1] Viboud C, Charu V, Olson D, Ballesteros S, Gog J, Khan F, et al. Demonstrating the use of high-volume electronic medical claims data to monitor local and regional influenza activity in the US. PloS one. 2014 jan;9(7):e102429.

[2] Cowling BJ, Fang VJ, Riley S, Peiris JSM, Leung GM. Estimation of the serial interval of influenza. Epidemiology. 2009;20(3):344–347.

[3] Cori A, Ferguson NM, Fraser C, Cauchemez S. A New Framework and Software to Estimate Time-Varying Reproduction Numbers During Epidemics. American Journal of Epidemiology. 2013;178(9):1505–1512.

[4] Biggerstaff M, Jhung M, Kamimoto L, Balluz L, Finelli L. Self-reported influenza-like illness and receipt of influenza antiviral drugs during the 2009 pandemic, United States, 2009-2010. Am J Public Health. 2012 oct;102(10):e21–26.

[5] Biggerstaff M, Jhung MA, Reed C, Fry AM, Balluz L, Finelli L. Influenza-like illness, the time to seek healthcare, and influenza antiviral receipt during the 2010-11 influenza season – United States. J Infect Dis. 2014;210(4):535–44.

[6] Mossong J, Hens N, Jit M, Beutels P, Auranen K, Mikolajczyk R, et al. Social contacts and mixing patterns relevant to the spread of infectious diseases. PLoS medicine. 2008 mar;5(3):e74.

[7] Chowell G, Miller MA, Viboud C. Seasonal influenza in the United States, France, and Australia: transmission and prospects for control. Epidemiology and infection. 2008;136(6):852–864.

[8] Mills CE, Robins JM, Lipsitch M. Transmissibility of 1918 pandemic influenza. Nature. 2004;432(December):904–906.

[9] Apolloni A, Poletto C, Ramasco JJ, Jensen P, Colizza V. Metapopulation epidemic models with heterogeneous mixing and travel behaviour. Theoretical biology & medical modelling. 2014;11(3):1–26.

[10] U S Department of Transportation BoTS. Air Carrier Statistics database: T-100 Domestic Market table; 2005.

[11] Apolloni A, Poletto C, Colizza V. Age-specific contacts and travel patterns in the spatial spread of 2009 H1N1 influenza pandemic. BMC Infect Dis. 2013 jan;13:176.

[12] Kucharski AJ, Conlan AJK, Eames KTD. School's Out: Seasonal Variation in the Movement Patterns of School Children. PloS one. 2015 jan;10(6):e0128070.